LARGE EDDY SIMULATION OF TURBULENT FLOW OVER A WALL UNDERGOING STREAMWISE TRAVELLING WAVE MOTION

Wuyang Zhang
Department of Engineering Mechanics
Tsinghua University
Beijing 100084, PR China
koala606@126.com

Weixi Huang
Department of Engineering Mechanics
Tsinghua University
Beijing 100084, PR China
hwx@tsinghua.edu.cn

Chunxiao Xu
Department of Engineering Mechanics
Tsinghua University
Beijing 100084, PR China
xucx@tsinghua.edu.cn

ABSTRACT

Turbulent channel flow with a wall undergoing travelling wave motion in streamwise direction was investigated using large eddy simulations at friction Reynolds number Re*=1000. Phase average and decomposition were used in the analysis of the flow field. Compared to flat wall turbulence, the large-scale motions in the outer layer are significantly enhanced by the traveling wave boundary. Obvious large-scale peaks in outer layer for all the three velocity components could be observed in the spanwise pre-multiplied energy spectra. A strengthened superposition effect of streamwise velocity fluctuation could also be seen in both energy spectra and conditionally averaged flow fields. The analysis of the two-point correlation function transport equation shows that the wave motion of the wall taking effect on the large-scale motion in the outer layer is mainly through the wave-induced production.

INTRODUCTION

The coupling dynamic processes between surface waves and turbulent flow are related to many complicated flow phenomena, such as the effect of the wind-induced wave to momentum flux at the ocean surface, and to the mixing and transport in the upper ocean. A fundamental understanding of the interaction of wave and turbulence is of significance in geophysics and ocean engineering. Existing researches show that turbulent flow over moving boundary has a significant difference with canonical flat plate boundary layer. For instance, Sullivan et al (2000) and Yang & Shen (2010) used the progressive wave wall as the idealized water wave and investigated the influence of wave to the momentum flux and coherence structures of turbulence.

In recent years, the large-scale motions scaled by the outer scale in the outer region of wall turbulence were found and confirmed at high Reynolds numbers (Kim & Adrain, 1999; Hutchins & Marusic, 2007a). Moreover, the influence of large-scale motions on near-wall fluctuations could be summarized to the superposition and modulation effects (Hutchins & Marusic, 2007b).

In the present work, we studied the turbulent flow over a traveling wavy wall by using large-eddy simulation and focused on the influence of the wavy boundary on the large-scale motions in the outer layer. In order to identify the wave-turbulence interactions, phase average and decomposition (Hussain & Reynolds, 1970) were used in the analysis of the flow field. The significantly enhanced effect on large-scale motions by wavy boundary could be observed in spanwise energy spectra of fluctuating velocity components and conditionally averaged flow fields. We also performed a spectral analysis of the two-point correlation function transport equation to investigate the mechanism of the wave motion of the wall effecting the large-scale motions in the outer layer.

PROBLEM FORMULATION AND NUMERICAL METHOD

The problem considered is a fully developed three-dimensional turbulent flow in a half channel over a wall undergoing traveling wave motion in the streamwise direction. A sketch of computational domain and coordinate system are shown in Figure 1. We adopt a Cartesian frame fixed in the physical space, with x, y and z

being the streamwise, vertical and spanwise coordinates (also denoted as x_1, x_2, and x_3). The corresponding velocity components in three directions are u, v, and w, respectively. A free-slip condition is applied on the upper boundary and a periodic condition in the streamwise and spanwise directions. The bottom wall undergoes a vertical oscillation in the form of the prescribed streamwise traveling wave. The flow is driven by an averaged streamwise gradient of pressure which is dynamically adjusted and makes the flow rate to be strictly constant in time. The Reynolds number based on the total drag (τ) and half channel width (δ) is about 1000. The wave steepness ak=0.1, where a is the wave amplitude, k is the wave number. Four wave phase speeds c are considered to investigate the effects of wave age. See Table 1 for the computational parameters.

In the present simulations, the filtered incompressible Navier-Stokes equation is solved by large-eddy simulation, and the subgrid-scale stress is modelled using the dynamic Smagorinsky model (Germano et al, 1991; Lilly 1992). The governing equations are integrated in time with a third-order time-splitting scheme. The accurate no-slip condition is satisfied at the wall by adopting the curvilinear coordinate system. A pseudo-spectral method in horizontal directions in conjunction with a second-order finite-difference method on a staggered grid in the vertical direction is used for spatial discretization. The computational domain size is $L_x \times L_y \times L_z = 4\pi\delta \times \delta \times 2\pi\delta$, and the corresponding grids are 288×144×288. The grid sizes in the two horizontal directions are uniform with the resolution that $\Delta x^+ \approx 45$, and $\Delta z^+ \approx 23$. The vertical grid sizes Δy^+ are changed from 0.05 near the bottom boundary to 10 near the top boundary.

Table 1. Computational parameters

ak	a^+	c/U_τ	Re_*
0	0	0	1045
0.1	53.49	0	1070
	51.91	7.3	1038
	48.35	15.4	987
	58.80	24.5	1176

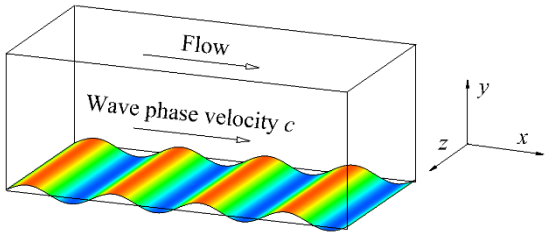

Figure 1. Computational domian and coordinate system.

RESULTS

In order to isolate the motions induced by wave and turbulence, the phase average (Hussain & Reynolds 1970) approach are used to quantify the statistical properties of the flow. A physical quantity can be decomposed as

$$f(x,y,z,t) = \bar{f}(y) + f_w(x,y) + f'(x,y,z,t), \qquad (1)$$

where $\bar{f}$, f_w, and f' are ensemble average, wave-induced, and turbulent components, respectively. In the later discussion, the ensemble and wave-induced component also referred as $[f]$ and $\tilde{f}$. A phase average over time, spanwise direction, and the same phase in the streamwise direction is defined as

$$\langle f \rangle(x,y) = \bar{f}(y) + f_w(x,y). \qquad (2)$$

The vertical profiles of the ensemble averaged streamwise velocity are shown in Figure 2. In the flat wall case (a^+=0), the mean velocity profile shows a classic logarithmic law beyond y^+>80. Similar to the flat wall case, all the profiles for waving wall cases with different phase speed also show a logarithmic law. The influence of wave to mean velocity profile is mainly on the roughness function (ΔU^+) which is decreasing with improved phase speed.

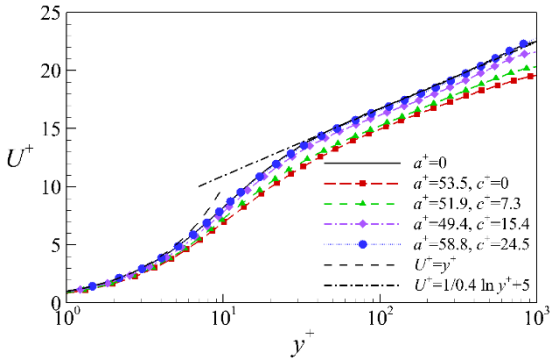

Figure 2. Mean velocity profile over wavy walls at different phase speed.

In order to investigate the effect of the travelling wave wall on the turbulent momentum flux transport, we can decompose the mean momentum flux into three components according to the definition of Eq (1),

$$\overline{uv} = \bar{u}\,\bar{v} + \overline{u_w v_w} + \overline{u'v'}. \qquad (3)$$

Where the second and the third term on the right-hand side are the wave-induced flux and the turbulent flux, respectively. Figure 3 shows the distributions of wave-induced fluctuating streamwise, vertical velocity and momentum flux for the stationary wavy wall, the vertical deformation of the wave wall is enlarged for showing the phase change clearly. The wave-induced streamwise velocity shown in Figure 3(a) has the positive fluctuation on the windward side of the wave and the negative fluctuation on the leeward side which means the fluid near the wall is accelerated at the windward face and decelerated at the leeward face. At the same time, the positive (negative) wave-induced vertical velocity also occur on the windward (leeward) side of the wave because of the fluid near the boundary moving along the wave surface. Near the surface, the streamwise and the vertical component are almost in the same phase resulting in negative pockets of the momentum flux $-u_w v_w$ centered slightly upstream of the crest and trough. Then the u_w contours tilt downstream with the vetical distance from the surface making the u_w and v_w become out phase and the corresponded momentum flux turn positive. This phenomenon reveals that the wave-induced velocity

fluctuation could affect the turbulent momentum flux transport in vertical direction. The strength of this wave-induced flux also changed with the phase of the wave as seen in Figure 3(c) which might affect the turbulent large-scale motions by turbulence transport mechanism as shown in the later.

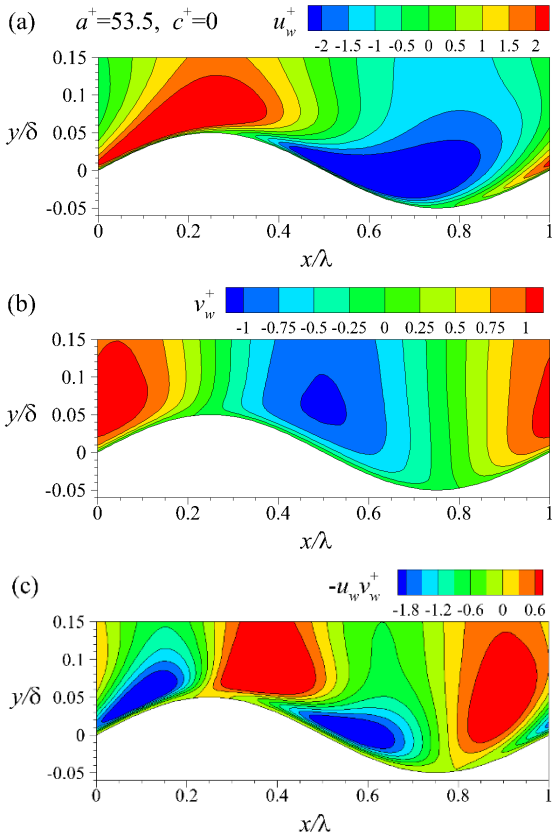

Figure 3. Wave-induced velocity fluctuation and momentum flux over stationary wavy wall: (a) u_w/u_τ; (b) v_w/u_τ; (c) $u_w v_w/u_\tau^2$.

Compared to the wave-induced fluctuations, the influence of the waving wall on vertical distribution of the turbulent velocity fluctuation is small, the results of that are not shown here. While the special scale distribution of the turbulent velocity fluctuation is extremely affected by the wave. The spanwise one-dimensional pre-multiplied energy spectra of streamwise, vertical and spanwise turbulent fluctuating velocity are shown in Figure 4. One distinct peak with the scale of $\lambda_z=2\delta$ can be clearly observed in the spanwise spectra for all the cases. For the streamwise velocity as shown in Figure 4(a) and (b), the peak in wavy boundary case is significantly strengthened compared to the flat wall case, especially for the stationary wavy wall. This large-scale fluctuation corresponds to the large-scale motion in the turbulence logarithmic region (Kim & Adrain, 1999; Hutchins & Marusic, 2007a). The peaks in the waving wall cases even extend from the logarithmic region into the near wall region at y^+=30 (Figure 4(a)), which indicates a strengthen superposition effect of the large-scale motion to near wall fluctuations (Hutchins & Marusic, 2007b). For the vertical velocity fluctuation, there is no large-scale peak for flat wall case in our simulation which conforms to other channel flow results at this low Reynolds number (Re_τ~1000), while a peak at scale $\lambda_z=2\delta$ appears in the stationary wavy wall case at the vertical location y/δ=0.5. The same phenomenon also could be seen in the spanwise velocity fluctuation, an additional large-scale peak appears at the vertical location about y^+~80. Therefore this result indicates the wavy wall could enhance the large-scale motions, while the effect vanished with improved phase speed.

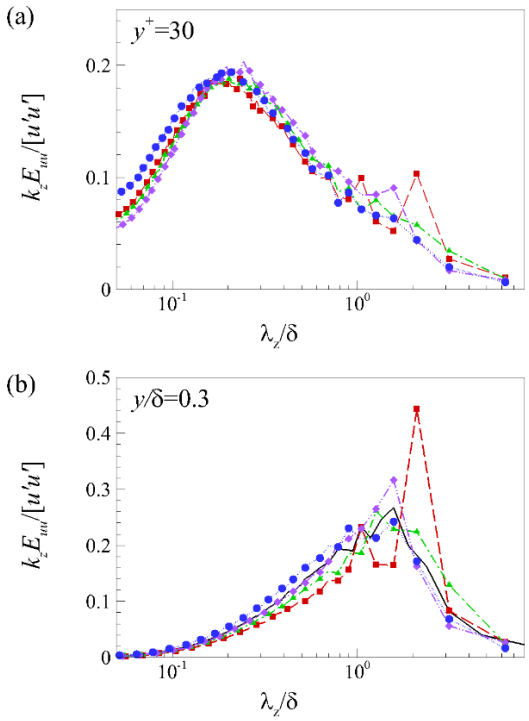

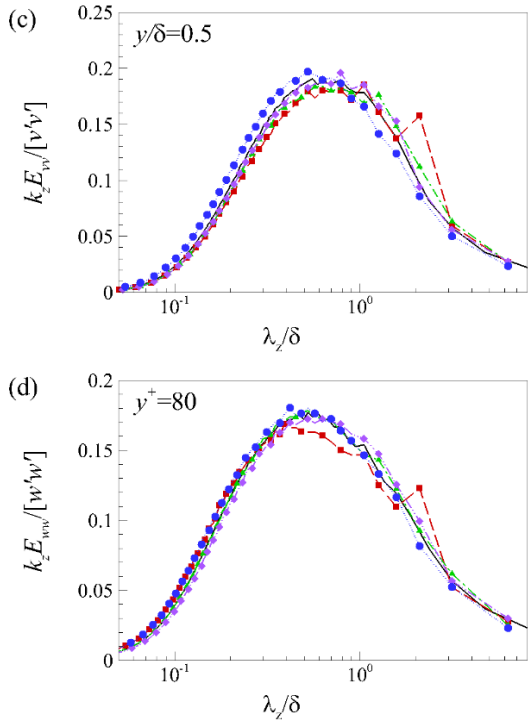

Figure 4. Spanwise 1D pre-multiplied energy spectra of fluctuating velocity: (a) u', y^+=30; (b) u', y/δ=0.3; (c) v', y/δ=0.5; (d) w', y^+=80. See Figure 1 for legend.

In order to visually observe the physical form of these large-scale motions, we used a conditional average for the large scale turbulent streamwise velocity fluctuation like Chung & Mckeon (2010). The condition chosen is set same for all the cases which is negative filtered large-scale ($\lambda_z>\delta$) streamwise velocity turbulent fluctuation ($u'_L<0$) at the referred vertical location is chosen at y^+=100. Figure 5 shows the 3-Dimensional flow fields, only flat wall case, and static wavy wall case are displayed. Under the same conditional average, the large-scale low momentum streaks are distinguished in both case, and the streak for wavy wall case is extremely longer than the flat wall case. We also intercept the vertical-spanwise plane at r_x=0 as shown in Figure 6. The positive and negative streamwise velocity contours in the section illustrate the large-scale flow structures are the large-scale low/high-speed streamwise streaks with the spanwise spacing of $\Delta z=\delta$ which scale is consistent with the large-scale peak in the spanwise spectral of velocity. And the cross velocity vectors in section revealed the large-scale streamwise roll cells between the streaks, these results also could be seen in the works of Chung & Mckeon (2010). Conforming to the energy spectra, the large-scale structures over the stationary wavy wall are stronger than those over the flat wall. Interestingly, the results shown here also had been reported in some experiments for static wavy wall (Günther et al, 2003; Kruse et al, 2003).

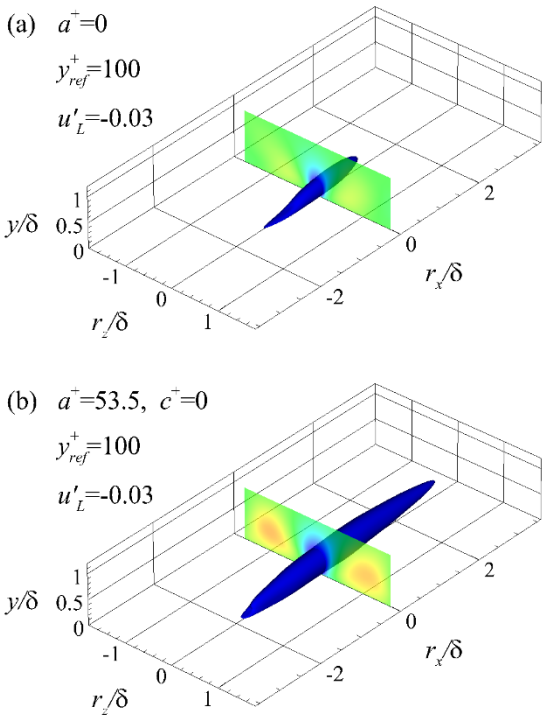

Figure 5. 3-Dimensional conditionally averaged flow fields: (a) flat wall; (b) stationary wave wall. The contour is large-scale streamwise velocity isosurface.

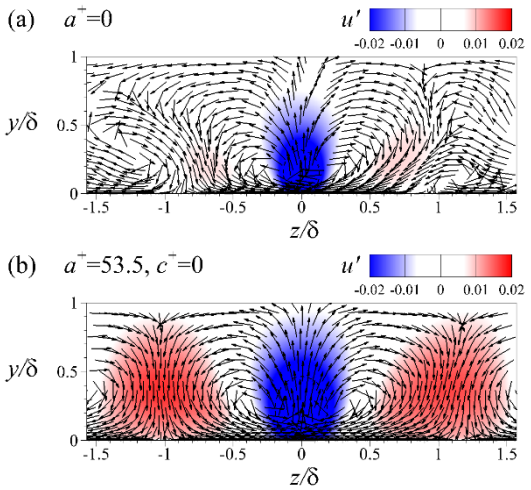

Figure 6. Vertical-spanwise sections of conditionally averaged flow fields: (a) flat wall; (b) stationary wave wall. Vectors represent in-plane velocity components.

The transport equation for two-point correlation function is an effect statistical method for analysing energy transfer between different scales. In present work, we referred to the experience of Lee & Moser (2015) and performed a spectral analysis of the transport equation for the spanwise two-point correlation function to explore the mechanism for the wavy wall influencing the turbulent fluctuation at different scales. Firstly, the equation for the velocity fluctuation in waving wall turbulence is,

$$\frac{\partial u_i'}{\partial t}+\left(\bar{u}_k+u_k'\right)\frac{\partial u_i'}{\partial x_k}+u_k'\left(\frac{\partial \bar{u}_i}{\partial x_k}+\frac{\partial u_i'}{\partial x_k}\right) = -\frac{\partial p'}{\partial x_i}+\frac{1}{Re}\frac{\partial^2 u_i'}{\partial x_k\partial x_k}-\frac{\partial}{\partial x_k}\left(u_i'u_k'-\left\langle u_i'u_k'\right\rangle\right)-\frac{\partial \tau_{ik}'}{\partial x_k}. \quad (4)$$

Where the τ_{ik}' is the subgrid-scale stress in large-eddy simulation. Then we define the velocity at the point with a certain distance in spanwise,

$$u_{jr}'=u_j'\left(x,y,z+r_z,t\right),\ \vec{x}_r=\left(x,y,z+r_z\right). \quad (5)$$

By multiplying Eq (4) by u_{jr}' and taking ensemble average, the transport equation for the spanwise two-point correlation function can be written as,

$$\partial_t\overline{u_i'u_{jr}'}\left(y,r\right)=P_{ij}+WP_{ij}+\Pi_{s,ij}+\Pi_{t,ij}+D_{ij}+T_{ij}+\varepsilon_{ij}. \quad (6)$$

Where,

$$P_{ij}=-\overline{u_{jr}'v'}\frac{\partial \bar{u}_i}{\partial y}-\overline{u_i'v_r'}\frac{\partial \bar{u}_j}{\partial y};$$

$$WP_{ij}=-\overline{u_{jr}'v'}\frac{\partial u_i'}{\partial y}-\overline{u_i'v_r'}\frac{\partial u_j'}{\partial y}-\left\langle u_{jr}'u'\right\rangle\left\langle\frac{\partial u_i}{\partial x}\right\rangle-\left\langle u_i'u_r'\right\rangle\left\langle\frac{\partial u_j}{\partial x}\right\rangle;$$

$$\Pi_{s,ij}=\overline{p'\frac{\partial u_{jr}'}{\partial x}}\delta_{i1}+\overline{p_r'\frac{\partial u_i'}{\partial x}}\delta_{j1}+\overline{p'\frac{\partial u_{jr}'}{\partial y}}\delta_{i2}+\overline{p_r'\frac{\partial u_i'}{\partial y}}\delta_{j2}+\overline{\frac{\partial p'u_{jr}'}{\partial r_z}}\delta_{i3}-\overline{\frac{\partial p_r'u_i'}{\partial r_z}}\delta_{j3};$$

$$\Pi_{t,ij}=-\overline{\frac{\partial p'u_{jr}'}{\partial x}}\delta_{i1}-\overline{\frac{\partial p_r'u_i'}{\partial x}}\delta_{j1}-\overline{\frac{\partial p'u_{jr}'}{\partial y}}\delta_{i2}-\overline{\frac{\partial p_r'u_i'}{\partial y}}\delta_{j2};$$

$$D_{ij}=\frac{1}{Re}\overline{\frac{\partial^2 u_i'u_{jr}'}{\partial x^2}}+\frac{1}{Re}\overline{\frac{\partial^2 u_i'u_{jr}'}{\partial y^2}};$$

$$T_{ij}=-\overline{\frac{\partial u_{jr}'\left(u_i'u'\right)}{\partial x}}-\overline{\frac{\partial u_i'\left(u_j'u'\right)_r}{\partial x}}-\overline{\frac{\partial u_{jr}'\left(u_i'v'\right)}{\partial y}}-\overline{\frac{\partial u_i'\left(u_j'v'\right)_r}{\partial y}}+\overline{u_i'u'\frac{\partial u_{jr}'}{\partial x}}+\overline{u_i'v'\frac{\partial u_{jr}'}{\partial y}}+\overline{\left(u_j'u'\right)_r\frac{\partial u_i'}{\partial x}}+\overline{\left(u_j'v'\right)_r\frac{\partial u_i'}{\partial y}}+\overline{\frac{\partial u_{jr}'\left(u_i'w'\right)}{\partial r_z}}-\overline{\frac{\partial u_i'\left(u_j'w'\right)_r}{\partial r_z}};$$

$$\varepsilon_{ij}=\frac{2}{Re}\overline{\frac{\partial u_i'}{\partial x}\frac{\partial u_{jr}'}{\partial x}}+\frac{2}{Re}\overline{\frac{\partial u_i'}{\partial y}\frac{\partial u_{jr}'}{\partial y}}-\frac{2}{Re}\overline{\frac{\partial^2 u_i'u_{jr}'}{\partial r_z^2}}.$$

The terms on the right-hand side of Eq (6) denote the production, wave-induced production, pressure-strain, pressure-transport, viscous transport, turbulent-transport, and dissipation respectively. For streamwise, vertical fluctuation and vertical momentum flux, the wave-induced production can be expressed as, respectively,

$$WP_{11}=-\overline{\left(u_r'v'+u'v_r'\right)\frac{\partial u}{\partial y}}-2\overline{\left\langle u'u_r'\right\rangle\left\langle\frac{\partial u}{\partial x}\right\rangle} =WP_{11,uy}+WP_{11,ux}; \quad (7)$$

$$WP_{22}=-\overline{\left(\left\langle u_r'v'\right\rangle+\left\langle u'v_r'\right\rangle\right)\left\langle\frac{\partial v}{\partial x}\right\rangle}-2\overline{\left\langle v'v_r'\right\rangle\left\langle\frac{\partial v}{\partial y}\right\rangle} =WP_{22,vx}+WP_{22,vy}; \quad (8)$$

$$WP_{12}=-\overline{v_r'v'\frac{\partial u}{\partial y}}-\overline{\left\langle u'v_r'\right\rangle\left\langle\frac{\partial v}{\partial y}\right\rangle}-\overline{\left\langle v_r'u'\right\rangle\left\langle\frac{\partial u}{\partial x}\right\rangle}-\overline{\left\langle u'u_r'\right\rangle\left\langle\frac{\partial v}{\partial x}\right\rangle} =WP_{12,uy}+WP_{12,vy}+WP_{12,ux}+WP_{12,vx}; \quad (9)$$

As can be seen that the wave-induced production term is the correlation of the wave-induced turbulent Reynolds stress and the velocity gradient and note that there is no production term for vertical fluctuation in the flat wall case. All the terms were further discretized in spectra space,

$$f\left(y,r_z\right)=\sum_{k_z}\hat{f}\left(y,k_z\right)\exp\left(\mathrm{i}k_zr_z\right). \quad (10)$$

Where the k_z are wavenumbers in spanwise direcitons. Then the one-dimensional energy spectra density of f can be defined as,

$$E_f\left(y,k_z\right)=\hat{f}\left(y,k_z\right)+\hat{f}\left(y,-k_z\right). \quad (11)$$

The contribution of each term to all scales fluctuation can be embodied in the spectra.

Figure 7 shows the spanwise one-dimensional premultiplied spectra of $WP_{11,uy}$, $WP_{22,vx}$ and $WP_{22,vx}$ for stationary wave wall case. The three terms we chose are the dominant items of their respective wave-induced production. For the first one, a positive peak can be identified in Figure 7(a) at spanwise scale $\lambda_z=2\delta$ and vertical location $y^+\sim30$, which indicates the streamwise large-scale motion could gain energy from the wave-induced velocity shear. While the distinct positive peaks corresponded to same large-scale while at outer region $y/\delta=0.5$ in Figure 7(b) and Figure 7(c) also illustrate the positive contribution of wave motion to large–scale vertical fluctuation and momentum flux. The vertical locations of the positive peaks in the spectral are consistent with the results of large-scale turbulent fluctuation as shown in Figure 4. Noteworthy, all the terms showed a negative region at small-scales in the inner region, this can be interpreted as the wave will make the small-scale turbulent motion in the inner region lost their energy. There is no additional wave-induced production term in the transport equation for spanwise velocity fluctuation and it is usually considered to gain energy from the pressure-strain term $\Pi_{s,33}$. In our simulation, the large-scale part of $\Pi_{s,33}$ is also strengthened in waving wall case.

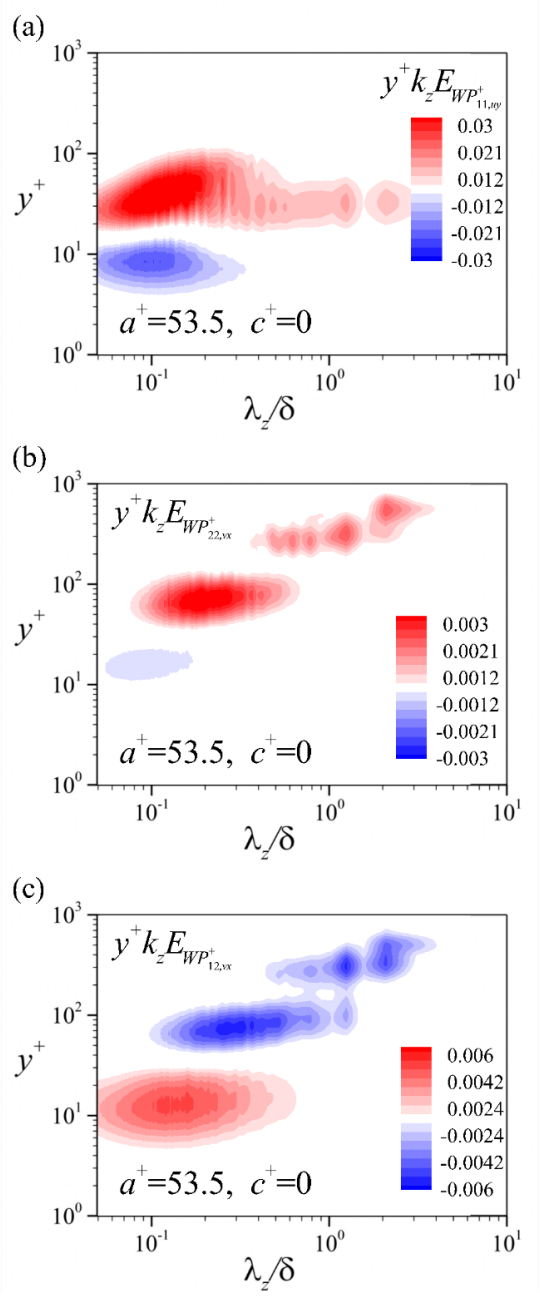

Figure 7. Spanwise 1D spectra density of wave-induced production for stationary wave wall case.

CONCLUSION

The present work, large-eddy simulation is used to simulate the turbulent channel flow with a wall undergoing travelling wave motion in streamwise direction. A special phase average and decomposition were applied in the flow fields to distinguish the fluctuation and momentum flux induced by wave and turbulence. From the statistical results, travelling wave boundary could change the spatial and scale distribution of fluctuation. The correlation of wave-induced velocity fluctuation can extremely affect the vertical momentum transport of flow. The large-scale turbulent velocity is enhanced by waving wall especially for static wavy wall and wave with low phase speed. The physical form of the large-scale motions was caught by conditional average. Their flow patterns and spatial scale consistent with the large-scale motion in the turbulence logarithmic region.

Investigation of the physical mechanisms responsible for the enhanced large-scale motions by spectra analysing of the transport equations of two-point correlation function. The results indicates that the wave-induced production defined as the correlation of the wave-induced Reynolds stress and velocity gradient has a special contribution to the large-scale motion. The influence of wavy boundary to turbulence is not only confined to the near-wall region also extends into the logarithmic region.

REFERENCES

Chung, Daniel, and B. J. McKeon. "Large-eddy simulation of large-scale structures in long channel flow." *Journal of Fluid Mechanics* 661 (2010): 341-364.

Germano, Massimo, Ugo Piomelli, Parviz Moin, and William H. Cabot. "A dynamic subgrid‐scale eddy viscosity model." *Physics of Fluids A: Fluid Dynamics 3*, no. 7 (1991): 1760-1765.

Günther, Axel, and Philipp Rudolf Von Rohr. "Large-scale structures in a developed flow over a wavy wall." *Journal of Fluid Mechanics* 478 (2003): 257-285.

Hussain, A. K. M. F., & Reynolds, W. C., 1970, "The mechanics of an organized wave in turbulent shear flow, " *Journal of Fluid Mechanics*, Vol. 41, 241-258.

Hutchins, N., & Marusic, I., 2007a, "Evidence of very long meandering features in the logarithmic region of turbulent boundary layers", *Journal of Fluid Mechanics*, Vol. 579, pp. 1-28.

Hutchins, N., & Marusic, I., 2007b, "Large-scale influences in near-wall turbulence", *Philosophical Transactions of the Royal Society of London A: Mathematical, Physical and Engineering Sciences*, Vol. 365, pp. 647-664.

Kim, K. C., & Adrian, R. J., 1999. "Very large-scale motion in the outer layer", *Physics of Fluids (1994-present)*, Vol. 11, pp.417-422.

Kruse, Nils, Axel GÜnther, and Philipp RUDOLF Von Rohr. "Dynamics of large-scale structures in turbulent flow over a wavy wall." *Journal of Fluid Mechanics* 485 (2003): 87-96.

Lee, Myoungkyu, and Robert D. Moser. "Spectral analysis on Reynolds stress transport equation in high Firewall-bounded turbulence." In *International Symposium on Turbulence and Shear Flow Phenomena (TSFP-9)*, pp. 4A–3. Melbourne. 2015.

Lilly, Douglas K. "A proposed modification of the Germano subgrid-scale closure method." *Physics of Fluids A: Fluid Dynamics 4*, no. 3 (1992): 633-635.

Sullivan, P. P., McWilliams, J. C., & Moeng, C. H., 2000, "Simulation of turbulent flow over idealized water waves", *Journal of Fluid Mechanics*, Vol. 404, pp.47-85.

Yang, D., & Shen, L., 2010, "Direct-simulation-based study of turbulent flow over various waving boundaries", *Journal of Fluid Mechanics*, Vol. 650, pp.131-180.